Supplementary Material

1 FREE VIBRATION ANALYSIS FOR THE FREE-FREE EULER-BERNOULLI BEAM

1.1 Natural frequencies and mode shapes

Considering an Euler-Bernoulli beam with two free ends, the governing equation for the motion of transverse free vibration reads Geradin and Rixen (2015)

$$\frac{\partial^2}{\partial z^2}(EI\frac{\partial^2 w}{\partial z^2}) + \rho A\frac{\partial^2 w}{\partial t^2} = 0, \tag{S.1}$$

with boundary conditions

$$\frac{\partial^2 w}{\partial z^2}\Big|_{z=0} = 0, \tag{S.2a}$$

$$\frac{\partial}{\partial z}(EI\frac{\partial^2 w}{\partial z^2})\Big|_{z=0} = 0, \tag{S.2b}$$

$$\frac{\partial^2 w}{\partial z^2}\Big|_{z=L} = 0, \tag{S.2c}$$

$$\frac{\partial}{\partial z}(EI\frac{\partial^2 w}{\partial z^2})\Big|_{z=L} = 0, \tag{S.2d}$$

where $w = w(z,t)$ is the lateral displacement of the beam. While E, A, ρ, L and I denote, respectively, Young's modulus, cross-section area, mass density, length and second moment of area of the beam.

Assuming a form of time-harmonic solution $w(z,t) = W(z)e^{i\omega t}$, Eq. (S.1) becomes

$$\frac{\mathrm{d}^2}{\mathrm{d}z^2}(EI\frac{\mathrm{d}^2 W}{\mathrm{d}z^2}) - m\omega^2 W = 0, \tag{S.3}$$

where $m = \rho A$ and ω denotes the angular frequency. For the uniform beam with constant cross- section, Eq. (S.3) can be written as

$$\frac{\mathrm{d}^4 W}{\mathrm{d}z^4} - k^4 W = 0, \tag{S.4}$$

where $k^4 = \frac{m\omega^2}{EI}$. The characteristic equation of Eq. (S.4) has the following simple form

$$\lambda^4 = k^4, \tag{S.5}$$

which gives four distinct roots:

$$\lambda_1 = k, \lambda_2 = -k, \lambda_3 = ik, \lambda_4 = -ik. \tag{S.6}$$

This immediately gives the general solution of Eq. (S.4):

$$W(z) = C_1\cos(kz) + C_2\sin(kz) + C_3\cosh(kz) + C_4\sinh(kz), \tag{S.7}$$

with four arbitrary constants C_n $(n = 1, 2, 3, 4)$. The condition for non-trivial solutions and boundary conditions Eq. (S.2) lead to the following transcendental equation:

$$\cos(\mu)\cosh(\mu) = 1, \tag{S.8}$$

with unknown $\mu = kL$. Roots of Eq. (S.8) μ_n $(n = 1, 2, 3, \cdots)$, correspondingly, k_n $(n = 1, 2, 3, \cdots)$, give the eigenvalues for Eq. (S.3), i.e., natural frequencies ω_n $(n = 1, 2, 3, \cdots)$ that we're interested in. For clarity, the first three zeros are illustrated in. Accordingly, the natural frequency of the transverse free vibration of the free-free Euler-Bernoulli beam becomes

$$w_n = \frac{\mu_n^2}{L^2}\sqrt{\frac{EI}{\rho A}},\ n = 1, 2, 3, \cdots. \tag{S.9}$$

After some tedious derivation, one can obtain the corresponding eigenmodes (i.e., the natural mode shapes) as follows

$$W_n(z) = \sin(\mu_n \frac{z}{L}) + \sinh(\mu_n \frac{z}{L}) + \frac{\sin(\mu_n) - \sinh(\mu_n)}{\cosh(\mu_n) - \cos(\mu_n)}\left[\cos(\mu_n \frac{z}{L}) + \cosh(\mu_n \frac{z}{L})\right],\ n = 1, 2, 3, \cdots. \tag{S.10}$$

1.2 Orthogonality of mode shapes

Orthogonality of eigenmodes is indispensable for the derivation of eigenvalue problems in the main text. For the constant cross-section beam, the orthogonality condition states that given any two eigenmodes $W_n(z)$ and $W_m(z)$, which correspond to two distinct eigenfrequencies ω_n and ω_m, the following equation holds true

$$\langle W_n, W_m \rangle = 0, \tag{S.11}$$

herein, for the sake of brevity, the inner product notation $\langle f, g \rangle$ was introduced to represent the integral of two functions f and g over the interval $[0, L]$, i.e.,

$$\langle f, g \rangle = \int_0^L f(z)g(z)\mathrm{d}z.$$

To proof this conclusion, we use the fact that both $W_n(z)$ and $W_m(z)$ satisfy Eq. (S.3), that is,

$$\frac{\mathrm{d}^2}{\mathrm{d}z^2}(EI\frac{\mathrm{d}^2 W_n}{\mathrm{d}z^2}) = \rho A \omega_n^2 W_n, \tag{S.12a}$$

$$\frac{\mathrm{d}^2}{\mathrm{d}z^2}(EI\frac{\mathrm{d}^2 W_m}{\mathrm{d}z^2}) = \rho A \omega_m^2 W_m. \tag{S.12b}$$

Taking the inner product of Eq. (S.12a) and W_m and that of Eq. (S.12b) and W_n, we obtain:

$$\left\langle W_m, \frac{\mathrm{d}^2}{\mathrm{d}z^2}(EI\frac{\mathrm{d}^2 W_n}{\mathrm{d}z^2}) \right\rangle = \left\langle W_m, \rho A \omega_n^2 W_n \right\rangle, \tag{S.13a}$$

$$\left\langle W_n, \frac{\mathrm{d}^2}{\mathrm{d}z^2}(EI\frac{\mathrm{d}^2 W_m}{\mathrm{d}z^2}) \right\rangle = \left\langle W_n, \rho A \omega_m^2 W_m \right\rangle. \tag{S.13b}$$

Applying the integration by parts to the left-hand side of Eq. (S.13), one may get

$$\left[W_m \frac{\mathrm{d}}{\mathrm{d}z}(EI\frac{\mathrm{d}^2 W_n}{\mathrm{d}z^2})\right]\Bigg|_0^L - \left[\frac{\mathrm{d}W_m}{\mathrm{d}z} EI \frac{\mathrm{d}^2 W_n}{\mathrm{d}z^2}\right]\Bigg|_0^L + \left\langle EI\frac{\mathrm{d}^2 W_m}{\mathrm{d}z^2}, \frac{\mathrm{d}W_n}{\mathrm{d}z}\right\rangle = \omega_n^2 \left\langle W_m, \rho A W_n \right\rangle, \quad \text{(S.14a)}$$

$$\left[W_n \frac{\mathrm{d}}{\mathrm{d}z}(EI\frac{\mathrm{d}^2 W_m}{\mathrm{d}z^2})\right]\Bigg|_0^L - \left[\frac{\mathrm{d}W_n}{\mathrm{d}z} EI \frac{\mathrm{d}^2 W_m}{\mathrm{d}z^2}\right]\Bigg|_0^L + \left\langle EI\frac{\mathrm{d}^2 W_n}{\mathrm{d}z^2}, \frac{\mathrm{d}W_m}{\mathrm{d}z}\right\rangle = \omega_m^2 \left\langle W_n, \rho A W_m \right\rangle. \quad \text{(S.14b)}$$

Subtracting Eq. (S.14b) from Eq. (S.14a) and imposing boundary conditions listed in Eq. (S.2), we have

$$0 = (\omega_n^2 - \omega_m^2) \left\langle W_n, \rho A W_m \right\rangle. \quad \text{(S.15)}$$

For uniform beam with constant cross-section, it immediately lead to the conclusion that for two distinct eigenfrequencies (i.e., $\omega_n \neq \omega_m$) Eq. (S.11) holds true.

For the case when $m = n$,

$$\left\langle W_n, \rho A W_n \right\rangle = \int_0^L \rho A [W_n(z)]^2 \mathrm{d}z = M_n,$$

where, obviously, M_n is some positive number. The transformation was introduced to get the normalized eigenmode $\widetilde{W}_{(n)}(z)$ as follows:

$$\widetilde{W}_{(n)} = \frac{W_n}{\sqrt{\left\langle W_n, \rho A W_n \right\rangle}}, \quad \text{(S.16)}$$

then, using Eq. (S.13), one can immediately obtain the following equation:

$$\left\langle \widetilde{W}_{(n)}, \frac{\mathrm{d}^2}{\mathrm{d}z^2}(EI\frac{\mathrm{d}^2 \widetilde{W}_{(n)}}{\mathrm{d}z^2}) \right\rangle = \omega_n^2. \quad \text{(S.17)}$$

In conclusion, the orthogonality of mode shapes can be expressed as

$$\left\langle \widetilde{W}_{(n)}, \rho A \widetilde{W}_{(m)} \right\rangle = \left\langle \widetilde{W}_{(m)}, \rho A \widetilde{W}_{(n)} \right\rangle = \delta_{nm}, \quad \text{(S.18a)}$$

$$\left\langle \widetilde{W}_{(n)}, \frac{\mathrm{d}^2}{\mathrm{d}z^2}(EI\frac{\mathrm{d}^2 \widetilde{W}_{(m)}}{\mathrm{d}z^2}) \right\rangle = \left\langle \widetilde{W}_{(m)}, \frac{\mathrm{d}^2}{\mathrm{d}z^2}(EI\frac{\mathrm{d}^2 \widetilde{W}_{(n)}}{\mathrm{d}z^2}) \right\rangle = \omega_n^2 \delta_{nm}, \quad \text{(S.18b)}$$

where $\widetilde{W}_{(n)}$ was defined through Eq. (S.16) and

$$\delta_{nm} = \begin{cases} 1, & n = m \\ 0, & n \neq m \end{cases}, \ (n, m = 1, 2, 3, \cdots).$$

2 CALCULATIONS OF BERRY CURVATURE AND VALLEY CHERN NUMBERS

This section presents details of the numerical calculation of Berry curvature and valley Chern numbers. Note that the two bands above the first bandgap have a degeneracy at Γ point, and so do the two bands above the second bandgap. Thus, we have to calculate the combined Chern numbers associated these degenerate bands Wang et al. (2015), using the eigenvectors obtained from theoretical model and the eigenmodes data of an A-type unit cell output from FEM respectively.

2.1 Theoretical model

As stated in the main text, our beam-spring model give rise to the eigenvalue problem expressed as:

$$\boldsymbol{K}(\boldsymbol{k})\boldsymbol{\psi} = \omega^2 \boldsymbol{M}\boldsymbol{\psi}, \tag{S.19}$$

where $\boldsymbol{k}$ is the Bloch-wave vector. Solving Eq. S.19 for wave vectors $\boldsymbol{k}$ within the first Brillouin zone, we obtain the dispersion diagram $\omega = \omega(\boldsymbol{k})$ and the eigenvectors $\boldsymbol{\psi}$. For the 2D $\boldsymbol{k}$-space spanned by the basis vectors $\boldsymbol{b}_1$ and $\boldsymbol{b}_2$, we use a $N_{k_1} \times N_{k_2}$ grid that covers the first Brillouin zone (see figure S1), with N_{k_1} and N_{k_2} being the number of grid points along $\boldsymbol{b}_1$ and $\boldsymbol{b}_2$, respectively. The eigenvector associated to the n-th band is then a vector field, $\boldsymbol{\psi}(\boldsymbol{k}) = \boldsymbol{\psi}_n(k1, k2)$ defined on a 2D discretized parametric domain.

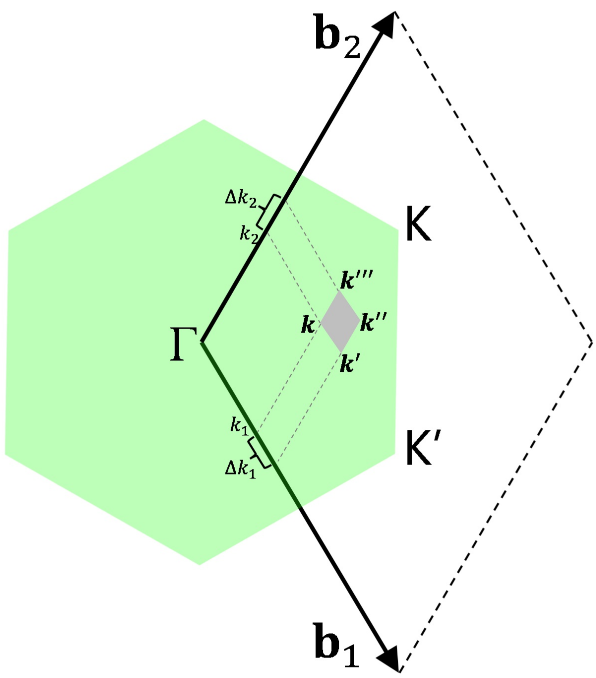

Figure S1. Schematic of a small patch (gray area) on the parallelogram spanned by basis vectors $\boldsymbol{b}_1$ and $\boldsymbol{b}_2$, which exactly covers the first Brillouin zone represented by the green hexagon region.

Following the procedure presented in Wang et al. (2015), we calculate the Berry flux associated to the n-th and m-th bands, $\widetilde{\mathcal{F}}_{mn}$, for a small patch of the size $\Delta k_1 \times \Delta k_2$ on the $\boldsymbol{k}$-grid:

$$\widetilde{\mathcal{F}}_{mn}(\boldsymbol{k}) = \ln\left(\frac{\boldsymbol{D}(\boldsymbol{k},\boldsymbol{k}')\boldsymbol{D}(\boldsymbol{k}',\boldsymbol{k}'')\boldsymbol{D}(\boldsymbol{k}'',\boldsymbol{k}''')\boldsymbol{D}(\boldsymbol{k}''',\boldsymbol{k})}{\boldsymbol{D}(\boldsymbol{k},\boldsymbol{k})\boldsymbol{D}(\boldsymbol{k}',\boldsymbol{k}')\boldsymbol{D}(\boldsymbol{k}'',\boldsymbol{k}'')\boldsymbol{D}(\boldsymbol{k}''',\boldsymbol{k}''')}\right), \tag{S.20}$$

where $\boldsymbol{k} = (k_1, k_2)$, $\boldsymbol{k}' = (k_1 + \Delta k_1, k_2)$, $\boldsymbol{k}'' = (k_1 + \Delta k_1, k_2 + \Delta k_2)$, $\boldsymbol{k}''' = (k_1, k_2 + \Delta k_2)$, and $\boldsymbol{D}(\boldsymbol{k}, \boldsymbol{k}')$ is the determinant of a 2×2 matrix expressed by:

$$\boldsymbol{D}(\boldsymbol{k}, \boldsymbol{k}') = \begin{pmatrix} \langle \boldsymbol{\psi}_n(\boldsymbol{k}), \boldsymbol{\psi}_n(\boldsymbol{k}') \rangle & \langle \boldsymbol{\psi}_n(\boldsymbol{k}), \boldsymbol{\psi}_m(\boldsymbol{k}') \rangle \\ \langle \boldsymbol{\psi}_m(\boldsymbol{k}), \boldsymbol{\psi}_n(\boldsymbol{k}') \rangle & \langle \boldsymbol{\psi}_m(\boldsymbol{k}), \boldsymbol{\psi}_m(\boldsymbol{k}') \rangle \end{pmatrix}, \tag{S.21}$$

where the inner product of two eigenvectors on the n-th and m-th bands is defined as:

$$\left\langle \boldsymbol{\psi}_n(\boldsymbol{k}), \boldsymbol{\psi}_m(\boldsymbol{k}') \right\rangle = [\boldsymbol{\psi}_n(\boldsymbol{k})]^\dagger \boldsymbol{\psi}_m(\boldsymbol{k}'). \tag{S.22}$$

Note that $\widetilde{\mathcal{F}}_{mn}$ in Eq. S.20 is defined within the principal branch of the logarithm function such that

$$-\pi < \frac{1}{i} \widetilde{\mathcal{F}}_{mn}(k_1, k_2) \leq \pi \quad \forall k_1, k_2. \tag{S.23}$$

Then the Berry curvature $\mathcal{F}_{mn}$ on this patch is defined as

$$\mathcal{F}_{mn}(\boldsymbol{k}) = \frac{i \widetilde{\mathcal{F}}_{mn}(\boldsymbol{k})}{\mathrm{d}S}, \tag{S.24}$$

where $\mathrm{d}S$ is the area of the small patch:

$$\mathrm{d}S = \left| \frac{\boldsymbol{b}_1}{N_{k_1}} \times \frac{\boldsymbol{b}_2}{N_{k_2}} \right|. \tag{S.25}$$

We calculate the combined Berry curvatures associated with the two bands above the first and second bandgap in MATLAB by setting $N_{k_1} = N_{k_2} = 100$. The results are shown in the left column of figure 4B in the main text. Finally, the valley Chern number can be evaluated by computing the numerical integration of the Berry curvature over the half of the first Brillouin zone:

$$C^{(v)} = \frac{1}{2\pi} \iint_{BZ(v)} \mathcal{F}_{mn}(\boldsymbol{k}) \mathrm{d}S = \frac{i}{2\pi} \sum_{k_1, k_2} \widetilde{\mathcal{F}}_{mn}(k_1, k_2), \tag{S.26}$$

with v being K or K'.

2.2 FEM

We perform the dispersion analysis of the periodical infinite structure in the commercial finite element software COMSOL Multiphysics by using one unit cell, whose Bloch modes corresponding to the bands of interest at uniformly discretized $\boldsymbol{k}$ points covering the first Brillouin zone are exported for subsequent processing. All calculation procedures are the same as the previous subsection, except that the eigenvectors used in Eqs. S.20, S.21 and S.22 need to be replaced with the corresponding Bloch modes, which can be expressed as

$$\boldsymbol{U} = \left[u_x^1, u_y^1, u_z^1, u_x^2, u_y^2, u_z^2, \ldots, u_x^n, u_y^n, u_z^n \right]^T, \tag{S.27}$$

with n being the total number of FE nodes of the unit cell model.

Along this path, the combined Berry curvatures associated with the two bands above the first and second bangap are shown in the right column of figure 4B in the main text, which are in good agreement with those obtained by theoretical model. Finally, the numerical valley Chern number can be evaluated by the same way as the previous subsection and almost the same results are obtained.

REFERENCES

Geradin M, Rixen DJ. *Mechanical Vibrations: Theory and Application to Structural Dynamics* (Wiley) (2015).

Wang P, Lu L, Bertoldi K. Topological Phononic Crystals with One-Way Elastic Edge Waves. *Physical Review Letters* **115** (2015) 104302. doi:10.1103/physrevlett.115.104302.